Food Chemistry 307 (2020) 125543

Contents lists available at ScienceDirect

Food Chemistry

journal homepage: www.elsevier.com/locate/foodchem

Effects of phosphate fertiliser on the physicochemical properties of Tartary buckwheat (*Fagopyrum tataricum* (L.) Gaertn.) starch

Weili Zhang[a,1], Qinghua Yang[a,1], Meijuan Xia[a], Wenming Bai[a], Pengke Wang[a], Xiaoli Gao[a], Xiangwei Gong[a], Baili Feng[a], Licheng Gao[a], Meiliang Zhou[b], Jinfeng Gao[a,*]

[a] Northwest A&F University, College of Agronomy/State Key Laboratory of Crop Stress Biology in Arid Areas, Yangling 712100, Shaanxi Province, China
[b] Institute of Crop Sciences, Chinese Academy of Agricultural Sciences, Beijing, China

ARTICLE INFO

Keywords:
Tartary buckwheat
Phosphate fertiliser
Starch properties

ABSTRACT

Phosphate fertilisation affects the growth, development and quality of Tartary buckwheat. In this study, the effect of different phosphorus levels, including 0, 15, 75, and 135 kg/ha (non-, low-, medium-, and high-phosphorus levels, respectively), on the characteristics of starch from Tartary buckwheat were investigated in 2015 and 2017. With increased phosphorus level, the median diameter of starch granules and the apparent amylose content initially decreased and then increased. All starch samples showed the features of A-type X-ray diffraction patterns. Starches under medium-phosphorus treatment showed higher relative crystallinity than those under non-phosphorus treatment, as well as the highest solubility, gelatinisation enthalpy and transmittance among all starches. Starches under low-phosphorus treatment exhibited higher pasting properties than those under non-phosphorus treatment. This research revealed that phosphorus treatments and year significantly affected the physicochemical properties of Tartary buckwheat starch, and can provide information for the applications of starch in the food and non-food industries.

1. Introduction

Tartary buckwheat (*Fagopyrum tataricum* (L.) Gaertn.) is a dicotyledonous cereal belonging to the family Polygonaceae. This plant originated in eastern Tibet or northwestern Yunnan in China and is cultivated mainly in southern China, northern India, Bhutan, and Nepal (Li, Li, & Ding, 2010). Tartary buckwheat grains contain various nutrients, whose main compounds are rutin, polyphenols, proteins, polysaccharides, dietary fibre, lipids, microelements, and macroelements. It is regarded as a nutraceutical food material and medicinal plant because of the health-promoting properties of its grains (Wang et al., 2017).

Starch is the major form of carbohydrates stored in Tartary buckwheat seeds and exists as granules (Li, Li, Zhang, & Liang, 2013). The starch content of Tartary buckwheat is around 70%. The characteristics of starch greatly affects the quality of Tartary buckwheat (Qin, Wang, Shan, Hou, & Ren, 2010). Tartary buckwheat starch, as a potential source of retrograded starch, is more resistant to hydration and hence to digestion, indicating that it may contribute to a low glycaemic response (Panlasigui et al., 1992). Thus, these products may have health benefits for diabetic individuals and those with normal glucose response by sustaining their energy level and prolonging their satiety (Lu, Donner, Yada, & Liu, 2012).

Phosphorus (P) deficiency leads to stomatal-conductance decline, photosynthesis-rate reduction, carbon and nitrogen metabolism abnormalities, carbohydrate accumulation and protein-synthesis inhibition, which all play important roles in the growth, development and quality of crops (Mesquita et al., 2018). P fertilization also significantly affects the functional characteristics of starches. Previous reports have indicated that starches from potato and banana, with increased P linked to the starch, the solubility, transparency, resistance to retrogradation and viscosity increased and the gelatinization temperature decreased, which has broadened the industrial applications of starches (Mesquita et al., 2018; Jane, Chen, Lee, Mcpherson, & Kasemsuwan, 1999; Noda et al., 2007; Lu et al., 2011; Leonel, Carmo, Fernandes, Franco, & Soratto, 2015). To date, few studies have focused on the effect of P fertilisation on Tartary buckwheat starch (Wang, Tang, Fu, Huang, & Zhang, 2016; Li et al., 2013; Lu et al., 2012). The present work aimed to reveal variations in starch morphology and quality and acquire information about their characteristics at different P levels, which may have future applications.

* Corresponding author.
E-mail addresses: 2016060037@nwsuaf.edu.cn (Q. Yang), fengbaili@nwsuaf.edu.cn (B. Feng), zhoumeiliang@caas.cn (M. Zhou), gaojf7604@126.com (J. Gao).
[1] Both authors contribute equally to this paper.

https://doi.org/10.1016/j.foodchem.2019.125543
Received 30 March 2019; Received in revised form 11 September 2019; Accepted 16 September 2019
Available online 30 September 2019
0308-8146/

2. Material and methods

2.1. Plant materials and cultivation

Tartary buckwheat were grown under four P levels including 0, 15, 75 and 135 kg/ha (non-, low-, medium-, and high-P levels) and the phosphate fertilizer was used as base manure at the experimental farm of the Northwest A&F University (109.7 E, 38.3 N, altitude 1080 m), Yulin, Shaanxi Province, China in 2015 and 2017. All groups were treated with potassium (K) 37.5 kg/ha and nitrogen (N) 90 kg/ha. The area has a temperate semi-arid continental monsoon climate with the mean temperature of 18.0 °C, minimum temperature of 3.1 °C, maximum temperature of 31 °C in 2015 and the mean temperature of 17.5 °C, minimum temperature of −0.6 °C, maximum temperature of 28.2 °C in 2017 during the growing season of Tartary buckwheat. Annual mean precipitation of approximately 400 mm. Sandy loam is the type of the local soil. The former crop was nursery to Tartary buckwheat. In this site, the soil pH value was 8.76 and the soil contained 0.15% total nitrogen, 1.82 mg/kg available phosphate, and 21.65 mg/kg available potassium. Field management was conducted in accordance with the technical regulations of local cultivation.

2.2. Starch isolation

Starches were extracted from Tartary buckwheat samples following a previously reported method (Zhang et al., 2019). The starch granules were then stored at 4 °C in airtight containers.

2.3. Observation of starch-granule morphology

Scanning electron microscopy (JSM-6360LV, Jeol, Japan) was performed to observe the starch-granule surface morphology, which were photographed at 2000-× magnification.

2.4. Granule-size analysis

The starch samples were suspended in water, and then a laser-diffraction particle-size analyser (Mastersizer 2000E, Malvern, England) was used to measure particle-size distribution.

2.5. Measurement of phosphorus and apparent amylose contents

The phosphorus content was determined according to Zhao, Jiang, Dan, and Luo (2010).

The amylose content of starch was determined using the method of Yang et al. (2018). The absorbance of solution of Tartary buckwheat starch was determined with a Blue Star B spectrophotometer (Lab tech Ltd, Beijing, China). Amylose content was calculated from the standard curves of amylose, and results are expressed as amylose percentage.

2.6. Determination of pasting properties

The pasting properties of starch samples were examined using a Rapid Viscosity Analyzer (RVA4500, Perten, Stockholm, Sweden). The viscosity profiles of starch were recorded using starch suspensions (14% moisture basis, a total weight of 28.0 g). The following heat-treatment program was used: 50 °C for 1 min, heated to 95 °C for 3.7 min, kept at 95 °C for 2.5 min, cooled to 50 °C for 3.8 min, and kept at 50 °C for 2 min (Gao et al., 2016).

2.7. Determination of thermal properties

The thermal properties of the starches were measured using a differential scanning calorimeter (DSC2000, TA instrument, United States). Starch samples (3 mg, dry basis) were weighed in aluminum pans, mixed with deionised water (6 μl) and sealed. The sealed pans were stored at room temperature for 2 h for equilibration and then heated to 110 °C at a rate of 10 °C /min. An empty aluminium pan served as a reference. The equipment was calibrated with indium. The transition temperatures (initial, peak, and conclusion) and enthalpy change (ΔH) of the gelatinised samples were determined (Uarrota et al., 2013).

2.8. X-ray diffraction (XRD) analysis

The XRD patterns of the starch samples were obtained with an X-ray diffractometer (D8 ADVANCE A25; Bruker, Germany). The starch samples were analysed from 4° to 60° (2θ) at a scanning speed of 8°/min and the conditions of use were 40 kV and 40 mA (Chao et al., 2014). Relative crystallinity (%) was calculated by using MDI Jade 6 software.

2.9. Determination of retrogradation

The retrogradation curve of starch pastes was obtained using the method of Chao et al. (2014).

2.10. Determination of water solubility

The solubility of the starch samples was determined at 60, 70, 80, and 90 °C according to Liu et al. (2016) and Choi, Kim, Park, Kim, and Baik (2009).

2.11. Determination of light transmittance

Light transmittance was determined according to Chao et al. (2014) with a Blue Star B spectrophotometer (Lab tech Ltd, Beijing, China) at 620 nm using distilled water as a control.

2.12. Statistical analysis

All data were analyzed using SPSS 19.0 (SPSS Inc., Chicago, IL, USA) and Origin software (version 7.5, Microcal Inc., Northampton, MA, USA). All data are expressed as the mean ± standard deviation. Significant differences were tested by Duncan's multiple range test ($p < 0.05$).

3. Results and discussion

3.1. Morphological characteristics of starch

Scanning electron microscopy was used to reveal whether there were significant changes in granule morphology at different phosphorus levels. From Fig. 1, all the starches extracted from the Tartary buckwheat presented similar polygonal shapes with smooth edges and spherical shapes with various sizes, regardless of the amount of phosphate-fertiliser treatment applied to the Tartary buckwheat. Mesquita et al. (2018) studied the morphology of banana starch granules and found that their shape did not change but had different sizes under diverse phosphate treatments. Moreover, in the present work, the starch-granule size under non-P treatment was larger than that under phosphate treatments and the reason may be that the increased P application has prolonged the grain filling, in which big starch granules could be decomposed into medium granules (Waduge, Xu, Bertoft, & Seetharaman, 2013).

3.2. Starch granule-size distribution

Table 1 presents the result of starch granule size tested with a laser-diffraction particle-size analyser. All Tartary buckwheat starches exhibited a greater population in the medium-size zone (from 5 μm to 15 μm). With increased phosphate-fertiliser level, the proportions of starch granules in the large-size zone (> 15 μm) and small-size zone

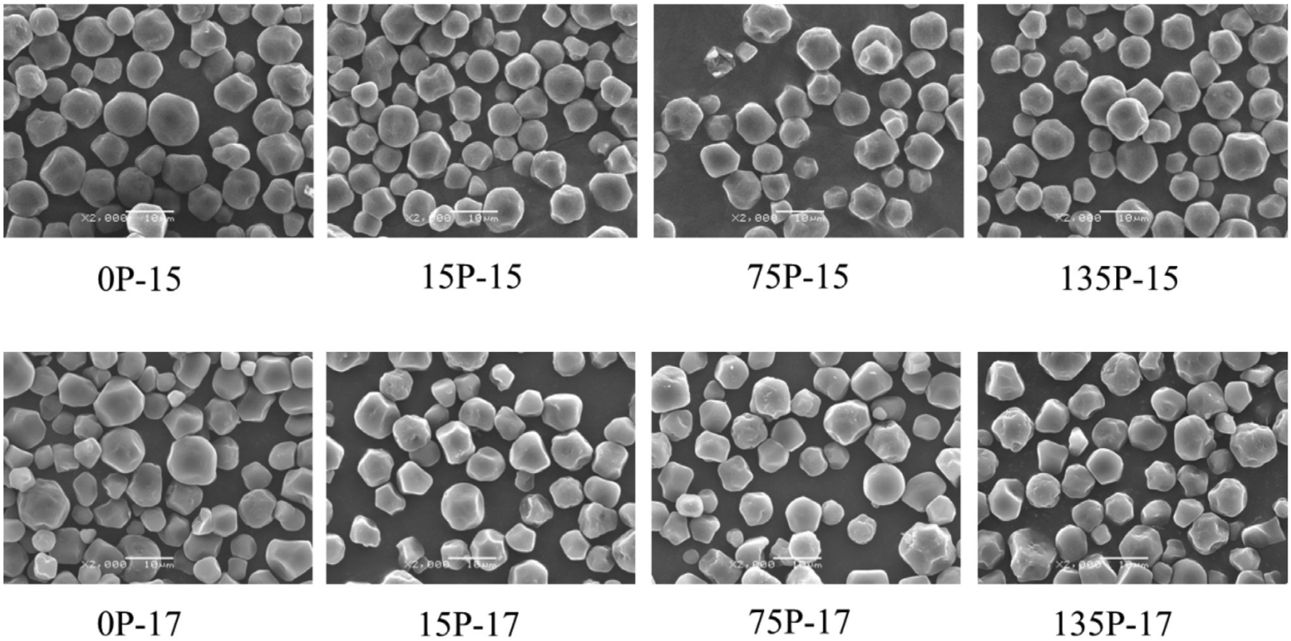

Fig. 1. The morphology of Tartary buckwheat starch granules under different phosphorus levels. The magnification is 2000× and Scale bar is 10 μm.

(< 5 μm) decreased and more starch granules with 5–15 μm diameters were observed. The phosphate-fertiliser application initially promoted the decrease in granules with median diameter, which then increased at the high-P level, consistent with the morphological characteristics observed by SEM. The median diameter of granules was the highest for starch from Tartary buckwheat with non-P treatment (9.83 μm in 2015 and 9.41 μm in 2017) and the lowest for starch from Tartary buckwheat at medium-P treatment (9.10 μm in 2015 and 9.93 μm in 2017). The variation in starch-granule size may be associated with the enzyme activity of starch biosynthesis in response to phosphate fertilization (Mesquita et al., 2018).

3.3. Phosphorus and apparent amylose contents of starch

In Table 1, there was a significant tendency for increased phosphorus content of starch with the increase of phosphate fertilisation application in Tartary buckwheat, which may be related to the phosphorus availability in the soil (Mesquita et al., 2018). In our experimental farm, the phosphorus availability was low and therefore it will activate the high affinity transporters in order to ensure the phosphorus can enter the cells.

With increased phosphate fertilisation, apparent amylose content initially decreased and then increased (Table 1). The starches under non-P treatment had the highest apparent amylose content, and the starches under medium-P treatment (75 kg/ha) had the lowest apparent amylose content in 2015 and 2017. The main reason for the decline was that the larger starch granules at non-P treatment included more long branch-chains of amylopectin than the smaller ones at medium-P treatment (Lindeboom, Chang, & Tyler, 2004). This result was in accordance with the above variation in median diameter of starch granules determined using a laser-diffraction particle-size analyser and may be explained by the activity of starch synthase (GBSS-I) (Mesquita et al., 2018; Wang et al., 2016; Utrilla-Coello, Agama-Acevedo, Paulina, Rodríguez-Ambriz, & Bello-Pérez, 2010). Tartary buckwheat with lower amylose content is expected to form less retrograded starch during hydrothermal-product processing while having good dough-kneading properties, which is particularly important in noodle making (Gao et al., 2016).

3.4. Pasting properties of starch

The parameters of pasting properties of Tartary buckwheat starches under different phosphate conditions are presented in Table 2. Pasting temperature is the temperature at which the viscosity of starch paste begins to rise (Kaur, Singh, Ezekiel, & Sodhi, 2009). The pasting temperature and pasting time of starches from different P treatments varied between 73.5 and 74.4 °C and 3.8 and 4.3 min, respectively. The highest pasting temperatures were observed for starches exposed to non-P treatment in 2015 and 2017 (Table 2). This finding indicated their great resistance to swelling, which may be influenced by amylose content,

Table 1
The Phosphorus content, granule size distribution and amylose content of Tartary buckwheat starch under different phosphorus levels.

Year	Phosphorus dose (kg/ha)	Phosphorus content	Median diameter	Granule size distribution (%)			Apparent amylose content (%)
		(%)		< 5 μm	5–15 μm	> 15 μm	
2015	0	0.068 ± 0.001c	9.21 ± 0.01a	6.19 ± 0.07a	84.38 ± 0.01d	9.43 ± 0.08a	26.99 ± 0.28a
	15	0.072 ± 0.001c	8.84 ± 0.04c	5.96 ± 0.10b	88.24 ± 0.03c	5.79 ± 0.13b	26.25 ± 0.16b
	75	0.081 ± 0.001b	8.69 ± 0.02d	4.81 ± 0.04d	91.64 ± 0.06a	3.55 ± 0.10c	24.73 ± 0.16d
	135	0.107 ± 0.004a	8.92 ± 0.00b	5.34 ± 0.01c	88.92 ± 0.08b	5.74 ± 0.10b	25.25 ± 0.04c
2017	0	0.067 ± 0.003c	10.13 ± 0.05a	6.83 ± 0.04c	73.12 ± 0.03d	20.05 ± 0.07a	28.58 ± 0.15a
	15	0.072 ± 0.001c	9.68 ± 0.04b	7.86 ± 0.08b	75.68 ± 0.01c	16.46 ± 0.10b	27.68 ± 0.21ab
	75	0.081 ± 0.001b	9.41 ± 0.00d	3.70 ± 0.03d	88.27 ± 0.08a	8.03 ± 0.11d	27.37 ± 0.12b
	135	0.108 ± 0.002a	9.55 ± 0.01c	8.05 ± 0.04a	76.55 ± 0.01b	15.40 ± 0.06c	27.39 ± 0.16b

Note: values in the same row with different superscripts mean significantly different ($p < 0.05$).

Table 2
The pasting properties, thermal properties and relative crystallinity of Tartary buckwheat starch under different phosphorus levels.

Year	Phosphorus dose (kg/ha)	Pasting properties							Thermal properties				Relative crystallinity (%)
		PV (cP)	TV (cP)	BD (cP)	FV (cP)	SB (cP)	PTM (°C)	Time (min)	To (°C)	Tp (°C)	Tc (°C)	ΔH (J/g)	
2015	0	5790 ± 25b	3874 ± 16b	1916 ± 40b	6386 ± 25c	2512 ± 41b	74.3 ± 0.0a	4.3 ± 0.0ab	65.07 ± 0.53a	68.88 ± 0.12a	74.74 ± 0.01a	8.75 ± 0.37c	27.08 ± 1.1b
	15	6300 ± 68a	4076 ± 52a	2225 ± 16a	6541 ± 31ab	2466 ± 20bc	73.5 ± 0.0b	4.2 ± 0.0b	64.68 ± 0.06a	68.28 ± 0.07b	73.25 ± 0.80b	9.17 ± 0.51bc	29.91 ± 0.4a
	75	5888 ± 36b	4039 ± 37a	1849 ± 1b	6436 ± 69bc	2397 ± 31c	74.3 ± 0.0a	4.3 ± 0.0a	64.42 ± 0.11a	68.43 ± 0.11b	74.67 ± 0.13a	11.04 ± 0.23a	30.34 ± 0.1a
	135	5870 ± 42b	3988 ± 6a	1882 ± 47b	6660 ± 40a	2672 ± 45a	73.5 ± 0.0b	4.1 ± 0.0c	64.44 ± 0.06a	68.46 ± 0.03b	74.44 ± 0.10a	10.07 ± 0.32ab	30.13 ± 0.1a
2017	0	6224c ± 34d	4150 ± 18d	2074 ± 16d	6976 ± 31c	2826 ± 13d	74.4 ± 0.1a	4.0 ± 0.0a	66.96 ± 0.08b	69.62 ± 0.06b	73.42 ± 0.40b	7.96 ± 0.12b	26.89 ± 0.1b
	15	6980 ± 25a	4365 ± 14b	2615 ± 11a	7312 ± 31b	2947 ± 17b	74.3 ± 0.0a	3.8 ± 0.1b	67.36 ± 0.08a	70.09 ± 0.00ab	74.72 ± 0.15a	10.55 ± 0.16a	31.42 ± 0.6a
	75	6634 ± 35c	4254 ± 25c	2380 ± 10b	7266 ± 33b	3012 ± 7a	73.5 ± 0.1b	3.9 ± 0.0b	67.34 ± 0.19a	70.67 ± 0.40a	75.02 ± 0.11a	10.70 ± 0.48a	31.89 ± 0.1a
	135	6830 ± 41b	4604 ± 17a	2226 ± 24c	7497 ± 32a	2893 ± 15c	74.3 ± 0.0a	3.8 ± 0.0b	64.99 ± 0.06c	68.81 ± 0.15c	74.91 ± 0.23a	10.64 ± 0.55a	31.43 ± 0.2a

Note: values in the same row with different superscripts mean significantly different ($p < 0.05$).
PV: peak viscosity; TV: trough viscosity; BD: breakdown viscosity; FV: final viscosity; SB: setback viscosity; PTM: pasting temperature; To: onset temperature; Tp: peak temperature; Tc: endset temperature; ΔH: enthalpy of gelatinization.

amylopectin molecular structure, and molecular weight (Jane et al., 1999). Peak viscosity refers to the maximum swelling value of starch granules during heating, and breakdown viscosity value is a measure of the degree of disintegration of granules and reflects the ability to resist heating (Shimelis, Meaza, & Rakshit, 2006; Kong, Zhu, Sui, & Bao, 2015). The peak viscosity and breakdown both increased to their highest levels at low-P treatment (15 kg/ha) in 2015 and 2017. The final viscosity, which is the degree of recovery of starch viscosity during cooling and reflects the interaction among leached amylose chains (Ambigaipalan et al., 2011). It was higher for the P-treated starches than for the non-P-treated ones.

3.5. Thermal properties of starch

The thermal properties of Tartary buckwheat starch during gelatinisation (To, Tp, Tc, and ΔH) are summarised in Table 2. Gelatinization temperature (onset and peak) can be used as a measure of stability or completeness of crystalline regions and the width of endothermic peak as an estimate of crystalline-structure heterogeneity (Blennow, Bay-Smidt, Olsen, & Moller, 2000). The onset temperature (To), peak temperature (Tp), and conclusion temperature (Tc) of all Tartary buckwheat starches ranged between 64.42 and 67.36 °C, 68.28 and 70.67 °C, and 73.25 and 75.02 °C, respectively. The temperature did not follow any trend in both years with amylose or P content. However, an increase in the enthalpy of gelatinisation was observed with increased phosphate fertiliser. Given that the crystalline regions of starch granules comprised mainly amylopectin, P enhanced the re-crystallisation of amylopectin (Lu et al., 2012). Similar results have been obtained in previous studies, i.e., amylose content of starches is low and the gelatinisation enthalpy of these starches is high (Leonel et al., 2015). The ΔH of native potato starch has also been observed to increase with increased P content (Karim et al., 2007). Enthalpy values were related to the molecular architecture of the crystalline region, amylose-to-amylopectin ratio, the presence of short amylopectin chains, the amount of double-helical order, and the molecular structure of amylose and amylopectin (Karim, Norziah, & Seow, 2000). Starches with higher and more perfect crystallinity have higher To and ΔH (Perera, Lu, Sell, & Jane, 2001).

3.6. XRD patterns of starch

The starches subjected to different P treatments all showed typical A-type XRD patterns (Fig. 2A, 2B), which had peaks at 15°, 17°, 18° and 23° (2θ). This finding revealed that different P treatments did not change the A-type XRD patterns of Tartary buckwheat starches. The peak positions of starches under different P fertilisers did not differ, but the intensities of all peaks exhibited small differences. Relative crystallinity initially increased and then decreased with increased P level, whereas no significant differences at low-, medium-, and high-P treatment were observed (Table 2). Starch granules have a non homogenous structure and consist of crystalline and amorphous regions (Ao & Jane, 2007). Amylopectin is generally known to be the dominant crystalline component in starch granules, while amylose weakens the crystal structure of amylopectin (Cheetham & Tao, 1998). In the present work, starches under non-P treatment had higher amylose content and lower relative crystallinity than the other starches. This result was similar to the previous findings in maze starch (Cheetham & Tao, 1998).

3.7. Retrogradation of starch

Starch endures chain-breaking when mixed and heated with water, and the interrupted starch chains then undergo recombination during the subsequent cooling, and this process is termed retrogradation (Wang, Li, Copeland, Niu, & Wang, 2015), which is related to the stability of a starch paste. The retrogradation rate of Tartary buckwheat starches presented a similar trend in 2015 and 2017 (Fig. 2C, 2D). The

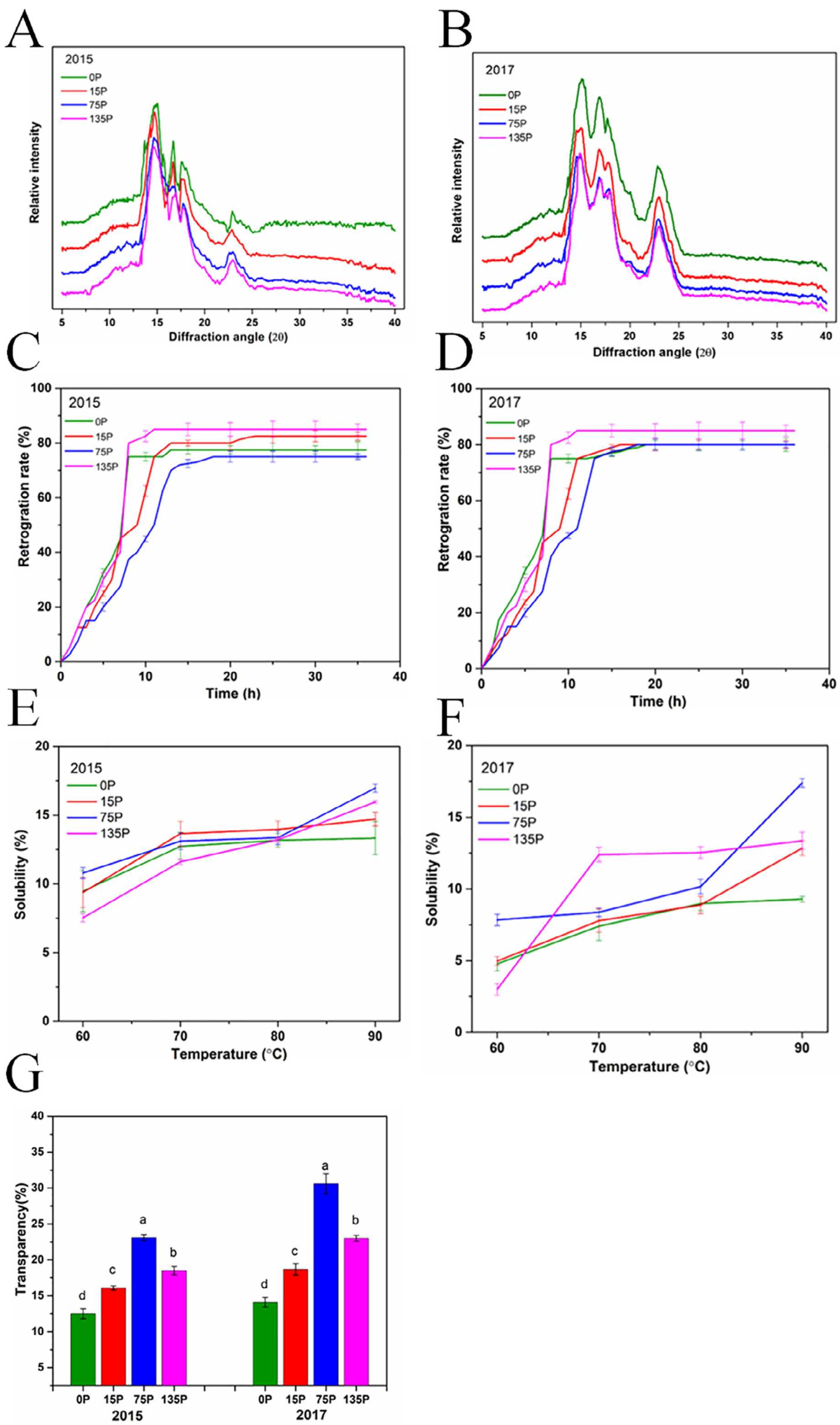

Fig. 2. The X-ray diffraction patterns, retrogradation, solubility and light transmittance of Tartary buckwheat starch under different phosphorus levels. (A), X-ray diffraction patterns of starch in 2015; (B), X-ray diffraction patterns of starch in 2017; (C), retrogradation of starch in 2015; (D), retrogradation of starch in 2017; (E), solubility of starch in 2015; (F), solubility of starch in 2017; (G), light transmittance of starch in 2015 and 2017. Note: values in the same year with different superscripts mean significantly different ($p < 0.05$).

retrogradation rate of starch pastes under P treatment of non-P (0 kg/ha) and high-P fertilisation (135 kg/ha) increased rapidly during the first 8 h and then gradually stabilised. Starch at high-P treatment had the highest retrogradation rates of 85%, whereas starch at medium-P treatment (75 kg/ha) had the lowest values of 75% in 2015 and 80% in 2017. In general, amylose is responsible for instantaneous retrogradation, and amylopectin is responsible for slow retrogradation of starch. This finding suggested that starches from Tartary buckwheat under high-P treatment had a higher proportion of very long-branched chains of amylopectin, because a high local concentration of longer unit chains could occur in the process of double-helix formation. In addition, the homogeneity in structure may speed the retrogradation rate. Notably, low retrogradation increases the digestive characteristics of starch (Colussi et al., 2017), decreases its hardness (Kingcam, Devahastin, & Chiewchan, 2008), and improves food quality (Fredriksson, Silverio, Andersson, Eliasson, & Åman, 1998).

3.8. Water solubility of starch

The water solubility of Tartary buckwheat starch at different phosphorus levels are summarised in Fig. 2E and 2F. The hydration of starch during heating reflect the magnitude of interaction among starch chains within the amorphous and crystalline domains (Karim et al., 2007). With increased temperature, the solubility of starches from Tartary buckwheat increased. The water solubility of starch under medium-P application (75 kg/ha) was the highest, whereas the water solubility of starch under non-P treatment (0 kg/ha) was the lowest. The difference in water solubility between 2015 and 2017 may be due to the smaller size of starch granules and the greater contact area with water in 2015, resulting in higher solubility. The variation in the molecular weight/distribution of amylose and amylopectin, the amylose-to-amylopectin ratio and the morphological structures of granules may also be responsible for the difference in water solubility of all starches (Singh & Singh, 2001).

3.9. Transparency of starch

The retrogradation of starch paste usually occurs during cooling and storage, and the decrease in the transparency of starch paste can reflect the retrogradation (Fukuzawa, Ogawa, Nakagawa, & Adachi, 2016). The results of transparency (%T) of starch pastes are presented in Fig. 2G. The transparency of Tartary buckwheat starch pastes significantly increased and then decreased in 2015 and 2017 with increased P treatment, indicating that appropriate P fertiliser application restrained starch retrogradation. Starch paste showed the highest light transmittances of 23.1% in 2015 and 30.6% in 2017 under medium-P fertilisation treatment (75 kg/ha), which was consistent with the results observed in Fig. 2C and 2D. Tester et al. also reported similar results that amylose content is negatively correlated with starch paste transparency in wheat starch (Tester & Karkalas, 2001). This result may be explained by the leaching of amylose chains out of the granules after cooling, which leads to the development of turbidity and decreased light transmittance in starch pastes (Wang et al., 2016).

3.10. Variance analysis and correlation analysis

The effect of phosphorus levels and years on physicochemical properties of Tartary buckwheat starch was investigated by means of analysis of variance. According to the result in the Table 3, the endset temperature and enthalpy of gelatinization were not affected by the years. In addition, the relative crystallinity and solubility at 60 °C were also not affected by interaction of treatments and years. However, treatments, years and the interaction of treatments and years all took significant effect on the other physicochemical properties of starch.

The correlations of physicochemical properties of Tartary buckwheat starch were analyzed using Pearson correlation analysis and are given in Fig. 3. The result in 2015 showed that the apparent amylose content had positive correlation with the proportion of starch granules (d < 5 μm), and onset temperature; meanwhile, there was significant negative correlation to enthalpy of gelatinization, light transmittance and solubility at 90 °C. In addition, a significant positive correlation among the apparent amylose content, median diameter and the proportion of starch granules (d > 15 μm), and a negative correlation among the apparent amylose content, the proportion of starch granules (d was 5–15 μm), endset temperature, enthalpy of gelatinization, relative crystallinity, light transmittance, solubility at 90 °C were observed in 2017. There were some differences in correlation coefficient in 2015 and 2017, which may be due to the differences in temperature, rainfall capacity and so on in these two years. This result is consistent with the finding using variance analysis.

Table 3
Effect of different phosphorus levels and years on physicochemical properties of Tartary buckwheat starch.

Variation		Treatments	Years	Treatments × years
DF		3	1	3
Apparent amylose content (%)		261.5**	1664.0**	33.0**
Granule size distribution (%)	Median diameter	273.6**	2418.0**	16.4**
	< 5 (μm)	1711.8**	1224.6**	785.3**
	5–15 (μm)	36146.2**	158080.2**	7766.6**
	> 15 (μm)	5860.1**	34018.6**	946.6**
Pasting properties	PV (cP)	167.4**	1219.3**	28.7**
	TV (cP)	81.3**	676.6**	45.4**
	BD (cP)	221.0**	784.0**	36.6**
	FV (cP)	73.2**	1536.3**	8.9*
	SB (cP)	12.4*	902.1**	41.7**
	PTM (°C)	120.1**	99.0**	340.7**
	Time (min)	25.3**	483.2**	4.1*
Thermal properties	To (°C)	36.0**	364.4**	25.8**
	Tp (°C)	21.7**	244.7**	29.4**
	Tc (°C)	6.2*	2.1	11.3**
	ΔH (J/g)	33.6**	1.1	6.7*
Relative crystallinity (%)		68.4**	19.7**	3.1
Transparency (%)		102.3**	88.7**	84.1**
Solubility	60 (°C)	18.9**	118.3**	1.1
	70 (°C)	4.9*	107.5**	18.0**
	80 (°C)	10.0**	178.6**	15.0**
	90 (°C)	55.7**	34.3**	14.9**

Note: "*" indicate statistical differences at $p < 0.05$, "**" indicate statistical differences at $p < 0.01$.
PV: peak viscosity; TV: trough viscosity; BD: breakdown viscosity; FV: final viscosity; SB: setback viscosity; PTM: pasting temperature; To: onset temperature; Tp: peak temperature; Tc: endset temperature; ΔH: enthalpy of gelatinization.

4. Conclusions

Starches under P treatment showed higher peak viscosity, trough viscosity, breakdown viscosity, final viscosity, and setback viscosity, as well as lower pasting temperature and pasting time, than starches under non-P treatment. P treatment did not change the XRD patterns. The relative crystallinity, gelatinisation enthalpy, solubility, and transmittance initially increased and then decreased, whereas the median diameter of starch granules and apparent amylose content initially decreased and then increased with increased P treatment. Overall, 75 kg/ha P treatment is recommended for Tartary buckwheat production.

Funding

This work was financially supported by the National Natural Science Foundation of China (31671631), Minor Grain Crops Research and Development System of Shaanxi Province (2016–2019), the Non-profit Industry (grain) Scientific Research Special Fund Agreement (no. 201513003-8) from the Ministry of Finance, People's Republic of China.

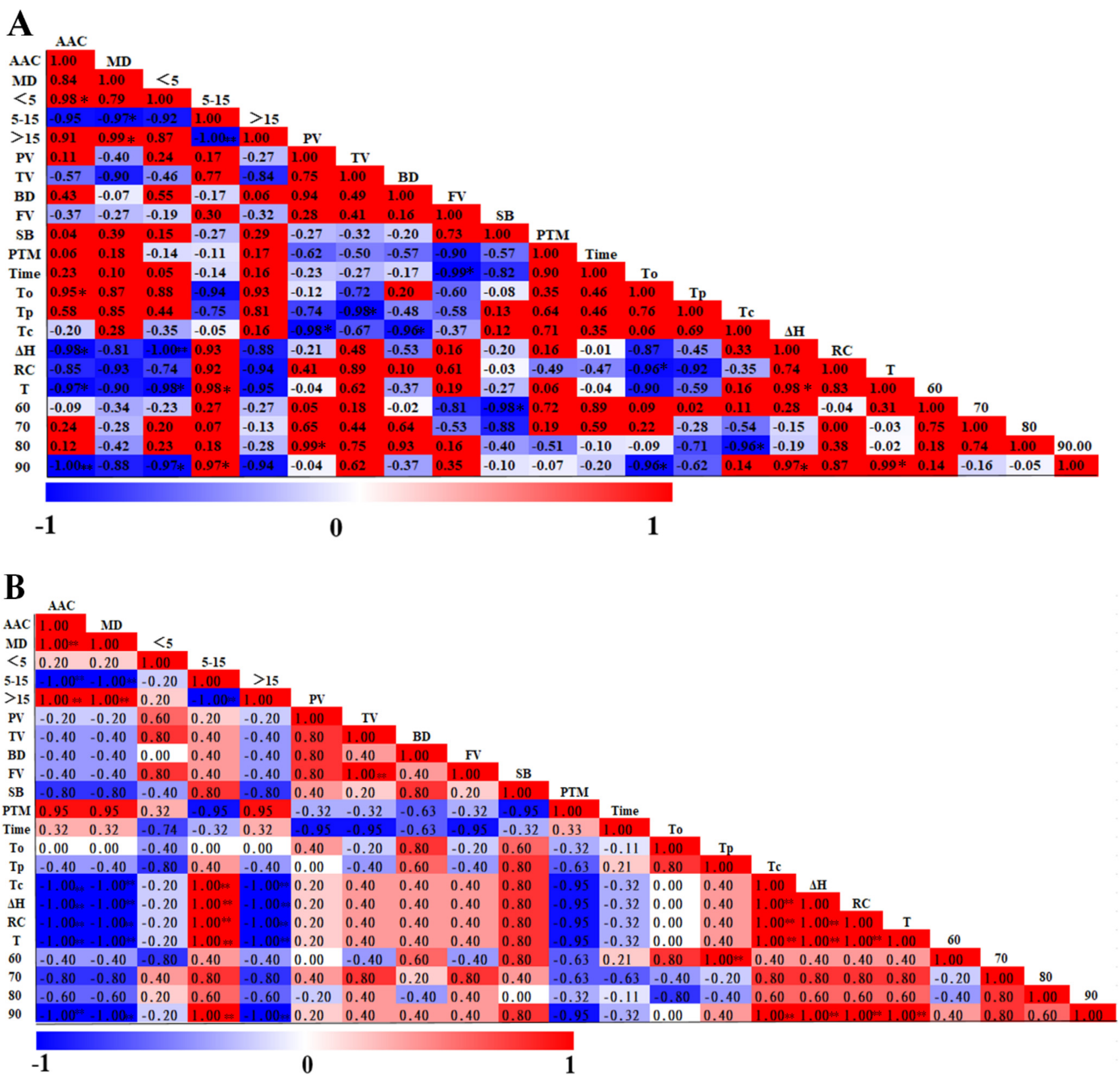

Fig. 3. Pearson correlation matrices of physicochemical properties of Tartary buckwheat starch. Data with single asterisk (*) and double asterisk (**) are statistically significant at P level < 0.05 and P level < 0.01, respectively. AAC: apparent amylose content; MD: median diameter; < 5: the proportion of starch granules of diameter less than 5 μm; 5–15: the proportion of starch granules of diameter from 5 to 15 μm; d > 15: the proportion of starch granules of diameter more than 15 μm; PV: peak viscosity; TV: trough viscosity; BD: breakdown viscosity; FV: final viscosity; SB: setback viscosity; PTM: pasting temperature; To: onset temperature; Tp: peak temperature; Tc: endset temperature; ΔH: enthalpy of gelatinization; RC: relative crystallinity; T: transparency; 60, 70, 80, 90: solubility at 60, 70, 80 and 90 °C.

Declaration of Competing Interest

The authors declare that they have no known competing financial interests or personal relationships that could have appeared to influence the work reported in this paper.

References

Ambigaipalan, P., Hoover, R., Donner, E., Liu, Q., Jaiswal, S., Chibbar, R., ... Seetharaman, K. (2011). Structure of faba bean, black bean and pinto bean starches at different levels of granule organization and their physicochemical properties. *Food Research International, 44*(9), 2962–2974.

Ao, Z., & Jane, J. L. (2007). Characterization and modeling of the a- and b-granule starches of wheat, triticale, and barley. *Carbohydrate Polymers, 67*(1), 46–55.

Blennow, A., Bay-Smidt, A. M., Olsen, C. E., & Moller, B. L. (2000). The distribution of covalently bound phosphate in the starch granule in relation to starch crystallinity. *International Journal of Biological Macromolecules, 27*(3), 211–218.

Chao, G. M., Gao, J. F., Liu, R., Wang, L., Li, C., Wang, Y., ... Feng, B. L. (2014). Starch physicochemical properties of waxy proso millet (*Panicum miliaceum* L.). *Starch-Starke, 66*, 1005–1012.

Cheetham, N. W. H., & Tao, L. P. (1998). Variation in crystalline type with amylose content in maize starch granules: An X-ray powder diffraction study. *Carbohydrate Polymers, 36*(4), 277–284.

Choi, H. S., Kim, H. S., Park, C. S., Kim, B. Y., & Baik, M. Y. (2009). Ultra high pressure (UHP)-assisted acetylation of corn starch. *Carbohydrate Polymers, 78*(4), 862–868.

Colussi, R., Singh, J., Kaur, L., Zavareze, E. D. R., Dias, A. R. G., Stewart, R. B., & Singh, H. (2017). Microstructural characteristics and gastro-small intestinal digestion in vitro of potato starch: Effects of refrigerated storage and reheating in microwave. *Food Chemistry, 226*, 171–178.

Fredriksson, H., Silverio, J., Andersson, R., Eliasson, A. C., & Åman, P. (1998). The influence of amylose and amylopectin on gelatinization and retrogradation properties

of different starches. *Carbohydrate Polymers, 35*(3–4), 119–134.
Fukuzawa, S., Ogawa, T., Nakagawa, K., & Adachi, S. (2016). Kinetics on the turbidity change of wheat starch during its retrogradation. *Bioscience Biotechnology and Biochemistry, 80*(8), 1–6.
Gao, J. F., Kreft, I., Chao, G. M., Wang, Y., Liu, X. J., Wang, L., ... Feng, B. L. (2016). Tartary buckwheat (*Fagopyrum tataricum* Gaertn.) starch, a side product in functional food production, as a potential source of retrograded starch. *Food Chemistry, 190*, 552–558.
Jane, J. L., Chen, Y. Y., Lee, L. F., Mcpherson, A. E., & Kasemsuwan, T. (1999). Effects of amylopectin branch chain length and amylose content on the gelatinization and pasting properties of starch 1. *Cereal Chemistry, 76*(5), 629–637.
Karim, A. A., Norziah, M. H., & Seow, C. C. (2000). Methods for the study of starch retrogradation. *Food Chemistry, 71*(1), 9–36.
Karim, A. A., Toon, L. C., Lee, V. P. L., Ong, W. Y., Fazilah, A., & Noda, T. (2007). Effects of phosphorus contents on the gelatinization and retrogradation of potato starch. *Journal of Food Science, 72*(2), 132–138.
Kaur, A., Singh, N., Ezekiel, R., & Sodhi, N. S. (2009). Properties of starches separated from potatoes stored under different conditions. *Food Chemistry, 114*(4), 1396–1404.
Kingcam, R., Devahastin, S., & Chiewchan, N. (2008). Effect of starch retrogradation on texture of potato chips produced by low-pressure superheated steam drying. *Journal of Food Engineering, 89*(1), 72–79.
Kong, X. L., Zhu, P., Sui, Z. Q., & Bao, J. S. (2015). Physicochemical properties of starches from diverse rice cultivars varying in apparent amylose content and gelatinisation temperature combinations. *Food Chemistry, 172*, 433–440.
Leonel, M., Carmo, E. L., Fernandes, A. M., Franco, C. M. L., & Soratto, R. P. (2015). Physico-chemical properties of starches isolated from potato cultivars grown in soils with different phosphorus availability. *Journal of the Science of Food and Agriculture, 96*(6), 1900–1905.
Li, C. Y., Li, C., Zhang, R. Q., & Liang, W. (2013). Effect of phosphorus on the characteristics of starch in winter wheat. *Starch-Starke, 65*(9–10), 801–807.
Li, D., Li, X. L., & Ding, X. L. (2010). Composition and antioxidative properties of the flavonoid-rich fractions from Tartary buckwheat grains. *Food Science and Biotechnology, 19*(3), 711–716.
Lindeboom, N., Chang, P. R., & Tyler, R. T. (2004). Analytical, biochemical and physicochemical aspects of starch granule size, with emphasis on small granule starches: A review. *Starch-Starke, 56*(3–4), 89–99.
Liu, H., Guo, X. D., Li, Y. L., Li, H. M., Fan, H. H., & Wang, M. (2016). In vitro digestibility and changes in physicochemical and textural properties of Tartary buckwheat starch under high hydrostatic pressure. *Journal of Food Engineering, 189*, 64–71.
Lu, Z. H., Donner, E., Yada, R. Y., & Liu, Q. (2012). The synergistic effects of amylose and phosphorus on rheological, thermal and nutritional properties of potato starch and gel. *Food Chemistry, 133*(4), 1214–1221.
Lu, Z. H., Yada, R. Y., Liu, Q., Bizimungu, B., Murphy, A., Koeyer, D. D., ... Pinhero, R. G. (2011). Correlation of physicochemical and nutritional properties of dry matter and starch in potatoes grown in different locations. *Food Chemistry, 126*(3), 1246–1253.
Mesquita, C.d. B., Garcia, É. L., Bolfarini, A. C. B., Leonel, S., Franco, C. M. L., & Leonel, M. (2018). Phosphate fertilization changes the characteristics of 'Maçã' banana starch. *International Journal of Biological Macromolecules, 112*, 1138–1145.
Noda, T., Kottearachchi, N. S., Tsuda, S., Mori, M., Takigawa, S., Matsuura-Endo, C., ... Yamauchi, H. (2007). Starch phosphorus content in potato (*Solanum tuberosum* L.) cultivars and its effect on other starch properties. *Carbohydrate Polymers, 68*(4), 793–796.
Panlasigui, L. N., Thompson, L. U., Juliano, B. O., Perez, C. M., Jenkins, D. J. A., & Yiu, S. H. (1992). Extruded rice noodles: Starch digestibility and glycemic response of healthy and diabetic subjects with different habitual diets. *Nutrition Research, 12*(10), 1195–1204.
Perera, C., Lu, Z., Sell, J., & Jane, J. (2001). Comparison of physicochemical properties and structures of sugary-2 cornstarch with normal and waxy cultivars 1. *Cereal Chemistry, 78*(3), 249–256.
Qin, P. Y., Wang, Q. A., Shan, F., Hou, Z. H., & Ren, G. X. (2010). Nutritional composition and flavonoids content of flour from different buckwheat cultivars. *International Journal of Food Science & Technology, 45*(5), 951–958.
Shimelis, E. A., Meaza, M., & Rakshit, S. K. (2006). Physico-chemical properties, pasting behavior and functional characteristics of flours and starches from improved bean (*Phaseolus vulgaris* L.) varieties grown in East Africa. *ICAE,* 8.
Singh, J., & Singh, N. (2001). Studies on the morphological, thermal and rheological properties of starch separated from some Indian potato cultivars. *Food Chemistry, 75*(1), 67–77.
Tester, R. F., & Karkalas, J. (2001). The effects of environmental conditions on the structural features and physico-chemical properties of starches. *Starch-Starke, 53*(10), 513–519.
Uarrota, V. G., Maraschin, M., Demiate, I. M., Amante, E. R., Delgadillo, I., & Vieira, F. (2013). Physicochemical, thermal, and pasting properties of flours and starches of eight brazilian maize landraces (*Zea mays* L.). *Food Hydrocolloids, 30*(2), 614–624.
Utrilla-Coello, R. G., Agama-Acevedo, E., Paulina, B. D. L. R. A., Rodríguez-Ambriz, S. L., & Bello-Pérez, L. A. (2010). Physicochemical and enzyme characterization of small and large starch granules isolated from two maize cultivars. *Cereal Chemistry Journal, 87*(1), 50–56.
Waduge, R. N., Xu, S., Bertoft, E., & Seetharaman, K. (2013). Exploring the surface morphology of developing wheat starch granules by using atomic force microscopy. *Starch-Starke, 65*, 398–409.
Wang, C., She, H. Z., Liu, X. B., Hu, D., Ruan, R. W., Shao, M. B., ... Yi, Z. L. (2017). Effects of fertilization on leaf photosynthetic characteristics and grain yield in Tartary buckwheat yunqiao1. *Photosynthetica, 55*(1), 77–84.
Wang, C., Tang, C. H., Fu, X., Huang, Q., & Zhang, B. (2016). Granular size of potato starch affects structural properties, octenylsuccinic anhydride modification and flowability. *Food Chemistry, 212*, 453–459.
Wang, S. J., Li, C. L., Copeland, L., Niu, Q., & Wang, S. (2015). Starch retrogradation: A comprehensive review. *Comprehensive Reviews in Food Science and Food Safety, 14*(5), 568–585.
Yang, Q. H., Zhang, P. P., Qu, Y., Gao, X. L., Liang, J. B., Yang, P., & Feng, B. L. (2018). Comparison of physicochemical properties and cooking edibility of waxy and non-waxy proso millet (*Panicum miliaceum* L.). *Food Chemistry, 257*, 271–278.
Zhang, W. L., Yang, Q. H., Xia, M. J., Bai, W. M., Wang, P. K., Gao, X. L., ... Gao, J. F. (2019). Effects of nitrogen level on the physicochemical properties of tartary buckwheat (*Fagopyrum tataricum* (L.) gaertn.) starch. *International Journal of Biological Macromolecules, 129*, 799–808.
Zhao, K., Jiang, S. J., Dan, Z., & Luo, C. H. (2010). Determination of phosphorus content in 350 cassava tuberous roots starch. *Journal of Anhui Agricultural Sciences, 38*(14), 7504–7505 7507.